Desalination and Water Treatment
www.deswater.com

doi: 10.5004/dwt.2019.23296

139 (2019) 360–368
January

Promising adsorption studies of bromophenol blue using copper oxide nanoparticles

M. Rashad[a,b,*], Hatem A. Al-Aoh[c]

[a]*Department of Physics, Faculty of Science, Assiut University, Assiut 71516, Egypt, Tel. +966-556061705, email: mohamed.ahmed24@science.au.edu.eg (M. Rashad)*
[b]*Nanotechnology Research Laboratory, Department of Physics, Faculty of Science, Tabuk University, Tabuk, Saudi Arabia*
[c]*Department of Chemistry, Faculty of Science, University of Tabuk, 71474 Tabuk, Saudi Arabia*

Received 11 February 2018; Accepted 17 October 2018

ABSTRACT

Nanoparticles (NPs) of copper oxide (CuO) were produced. Some physical properties of the prepared CuO NPs were investigated using XRD, TEM and BET surface analyzer techniques. pH at zero point charge (pH_{ZPC}) of the synthesized CuO NPs was also determined. The specific surface area, total pore volume, average pore diameter and pH_{ZPC} were found to be 6.188 mg/g, 0.0128 cm^3/g, 116.134 Å and 7.6, respectively. Adsorption of bromophenol blue (BB) on CuO NPs as adsorbent was conducted at various temperatures. The impacts of experimental conditions such as the primary concentration of BB solution, solution pH, agitation time and temperature were investigated. The adsorbate concentration of 300 mg/L, temperature of 60°C, 4h and pH of 1 were observed to be the ideal experimental conditions. Adsorption isotherm constants were investigated using the isotherm models of Langmuir and Freundlich. The data of this adsorption fits greatest to the isotherm model of Langmuir. The equilibrium amounts of BB uptake onto the surface of CuO NPs were found to be 20.19, 30.32 and 49.85 mg/g at 303, 318 and 333 K, in that order. The data of experimental kinetic were examined by the kinetic models of pseudo-first-order, second-order and intra-particle diffusion. The results of kinetic studies designate that the obtained data can be expressed well by the first-order kinetic model. Parameters of the thermodynamic were determined and their values indicate that the adsorption of BB by CuO NPs is un-spontaneous and endothermic processes.

Keywords: CuO nanoparticles; Bromophenol blue dye; Adsorption; Isotherm; Kinetics; Thermodynamics

1. Introduction

Metal oxides nanoparticles have attractive aspects in recent years because of their unique properties such as a large surface area, increased activity, electronic properties [1–3]. Among these transition metal oxides, nanoparticles of copper (II) oxide (CuO NPs) currently have significant interest due to their attractive properties [4]. It is superconductor for the temperature at critical and higher degrees, a semiconducting material and gas sensing metal oxide [4]. Therefore, various methods have been applied for production and characterization of CuO NPs. For example, wet chemical precipitation technique by maxing polyvinylpyrrolidone and copper nitrate in distilled water [5], microwave irradiation method [6], novel sol-gel method by adding copper chloride hex hydrates to acetic acid [7], chemical route method by calcination at a higher temperature [8], sol-gel method via maxing copper sulphate with sodium hydroxide [9] and inexpensive sol-gel route technique using various solvents [10] have been used for synthesis of CuO NPs. Due to rarely chemical and physical properties of CuO, it has an extensive range of applications in various technological areas such as a sensor for relative humidity [11], electrochemical measurements of dopamine [12] and extremely promising electrode [13]. Moreover, CuO NPs has been used as antimicrobial agent anti hydrophila of Aeromonas [14].

*Corresponding author.

In wastewater treatment, metal oxide NPs as general was employed as photocatalytic for degradation of methyl red [15] and methyl orange [16,17]. Photocatalytic degradation of dyes and formation reaction of C–N bond using Cu_2O and CuO nanoparticles were examined by Bhosale et al. [18]. Furthermore, CuO-nano-clinoptilolite has been applied for photodecolorization of methylene blue and bromophenol blue mixture [19]. All of these photocatalytic degradation studies designated that CuO NPs has significant catalytic effects towards the dyes photodegradation. In addition, methylene blue [20] and methyl orange [21] was removed from solutions by adsorption onto CuO NPs.

Dye of Bromophenol blue (BB) as a phenolic material has toxic, carcinogenic and teratogenic effects [22]. Therefore, the industrial wastewater related to the production and usages of BB are contaminated by this hazard dye. Thus many techniques have been used for elimination of BB from industrial wastewaters before their discharge into the environment. For example, solvent sublation method [23,24], photocatalytic degradation using $K_2Cr_2O_7$ [25] and TiO_2 nanoparticles [26] were employed to minimize this dye from wastewater. Moreover, various adsorbents such as chitosan composite [27], polymeric gels [28], mesoporous hybrid gel [29] and novel supported ionic liquids [30] were applied for removal of BB from polluted wastewater. CuO NPs was used to adsorb methylene blue and methyl orange from solutions [20,21] and for methylene blue [19]. Despite superior adsorptive-properties of CuO NPs towards methylene blue and methyl orange, there are no any attempt has been carried out to study BB adsorption from solution onto CuO NPs.

Thus the present work aims to study the adsorption performance of CuO NPs towards BB. Preparation and characterization of CuO NPs were performed. Consequently, isotherm, kinetics and thermodynamic parameters of BB adsorption on CuO NPs have been determined in a system of batch adsorption. Moreover, study the effect of some experimental conditions such as initial dye concentration, pH of solution, both temperature and agitation time on the adsorption capacity for the CuO NPs as an adsorbent.

2. Methodology

2.1. Synthesis and characterization of CuO NPs

For preparation CuO NPs, 0.2 M $Cu(NO_3)_2{\cdot}6H_2O$ was mixed with water solution containing 0.2 M $CO(NH_2)_2$. Then transfer to a microwave oven with 650 W power for 20 min [31,32]. The precipitated powder was centrifuged then washed using distilled water. The final products were collected for characterizations. X-Ray diffraction (XRD) measurements of Shimadzu XD-3A X-ray diffractometer at the 2θ range from 30 to 60, with monochromatized CuKα radiation (λ = 0.15418 nm) were used. Transmission electron microscopy (TEM) images were recorded on a JEOL-JEM 200CX model. The method of batch equilibrium [33] is used for measure the pH at the point of zero charge (pH_{ZPC}). The surface area and porosity of CuO NPs were analyzed by adsorption-desorption of N_2 at 758.58 mm Hg and 77.40 deg K using BET surface analyzer (NOVA-3200 Ver.6.09).

2.2. Adsorption procedures

Experiments related to the adsorption of BB dye onto CuO NPs were conducted by batch system. A 1000 mL of BB solution (1000 mg/L) was prepared then diluted to a fixed concentration of the working solutions. A 10 mL of solution was added to 25 mL amber bottle which has a fixed amount of CuO NPs (0.02 g). The bottles were then agitated at a constant rotation speed (150 rpm) and desired experimental conditions.

After the required shaking time, the adsorbent in each bottle was separated by Whattman filter paper. The remained concentrations of BB in the filtrate were quantified by 6800UV-spectrophotometer (Jenway) at λ_{max} of 590 nm. The masses of BB adsorbed per unit of CuO NPs (q in mg/g) at any time and equilibrium were computed from Eqs. (1) and (2), respectively [34].

$$q_t = \left(C_i - C_t\right)\frac{V}{W} \tag{1}$$

$$q_e = \left(C_i - C_e\right)\frac{V}{W} \tag{2}$$

q_t: BB quantities adsorbed at time (t) (mg/g), q_e: equilibrium BB quantities adsorbed (mg/g), C_i BB solution initial concentration (mg/L), C_t: adsorbate concentrations at time (t) (mg/L), C_e: equilibrium adsorbate concentrations (mg/L), V: adsorbate solution volume (L), W: adsorbent mass (g). Adsorptions of 45, 75 and 150 mg/L of this dye solution onto CuO NPs at various interval time periods were conducted to optimize agitation time, determine equilibrium contact time and to investigate the aspects of adsorption kinetics. The kinetic experimental data were also analyzed by pseudo-first order [Eq. (3)], pseudo second-order [Eq. (4)] and intraparticle diffusion [Eq. (5)] kinetic models [34].

$$\log\left(q_e - q_t\right) = \log q_e - K_1\frac{t}{2.303} \tag{3}$$

$$\frac{t}{q_t} = \frac{1}{K_2 q_e^2} + \frac{t}{q_e} \tag{4}$$

$$q_t = K_{dif}\sqrt{t} + C \tag{5}$$

K_1: pseudo-first order constants (min^{-1}), K_2: pseudo-second order constants (g/mg·min), K_{dif} intraparticle diffusion kinetic model $(mg/g{\cdot}min)^{1/2}$. C is a kinetic parameter constant which provides an idea of the boundary-layer thickness [35]. To study the impacts of adsorbate initial concentration, solution temperature and to analysis parameters of the isotherms along with thermodynamics, adsorption of BB solutions with concentrations in the range of 35–600 mg/L were carried out for 72 h at three different temperatures (303, 318 and 333 K). The equilibrium experimental data were explored by the Langmuir [Eq. (6)] linear forms and adsorption isotherm of Freundlich models [Eq. (7)]. The fundamental characteristics of Langmuir isotherm model were examined by the factor (R_L). The values of R_L were calculated using Eq. (6) [34].

$$\frac{C_e}{q_e} = \frac{1}{q_{max}K_L} + \frac{C_e}{q_{max}} \tag{6}$$

$$\ln q_e = \ln K_F + \frac{1}{n}\ln C_e \quad (7)$$

$$R_L = \frac{1}{1+K_L C_i} \quad (8)$$

q_{max}: maximum adsorption capacity (mg/g), K_L: Langmuir constant, K_F: Freundlich constant correlated to capacity of the adsorption, $1/n$: Freundlich constant corresponded to the favorability of adsorption. The adsorption is favorable when the value of 1/n lies between 0 and 1 [36]. K_L: Langmuir constant and C_i: maximum concentration of adsorbate. R_L value suggests the nature of isotherm, either favorable ($0< R_L < 1$), unfavorable ($R_L >1$), linear ($R_L = 1$), or irreversible ($R_L = 0$).

Thermodynamic parameters (ΔH°, ΔS° and ΔG°) were computed using Eqs. (9) and (10) [34].

$$\ln K_c = -\frac{\Delta H^o}{RT} + \frac{\Delta S^o}{R} \quad (9)$$

$$\Delta G^o = \Delta H^o - T\Delta S^o \quad (10)$$

T: temperature of solution (K), R: universal gas constant (8.314 J/K mol).

To understand the effect of pH solution on the adsorption of BB on CuO NPs, 0.1 N HCl and 0.1 N NaOH solutions were used to adjust solution pH. Adsorptions of 10 mL of 200 mg/L BB solutions with various initial pH values (1–7) were performed at room temperature and equilibrium contact time. The maximum wavelength of BB will be changed at pH over 7. Therefore, the impact of pH solution has been only investigated in this range (1–7).

3. Results and discussion

3.1. CuO NPs characterization

Fig. 1 presents XRD for CuO NPs. The intensities and angular peak positions are in good agreement with corresponding values [31]. In order to understand the phase symmetry of the prepared CuO NPs, a systematic study on the XRD was performed. Sharp peaks were obtained at angles corresponding to the planes (100), (002), (111), (20$\bar{2}$), (020) and (202). This indicates the structure of CuO nanocrystals [32] which was found to be highly crystalline. The average size of the both nanocrystals is estimated according to the following Debye-Scherer formula [37]:

$$D = \frac{K\lambda}{\beta cos\theta} \quad (11)$$

K = 0.94, λ: X-ray wavelength. β: diffraction peak full width at half maximum corresponding to 2θ. Using Eq. (11), the calculated crystallite sizes equal to 14 ± 1 nm for CuO NPs. Both size and internal morphology of the resultant CuO NPs are illustrated using transmission electron microscopy (TEM). Fig. 2 shows the TEM image of the prepared CuO NPs. TEM image presents that CuO NPs are spherical shapes with a narrow size distribution. It is obtained that the 10 ± 2 nm CuO particle size. Moreover, the, total pore volume, average pore diameter, surface area and pH_{ZPC} of this adsorbent are 0.0128 cm^3/g, 116.134 Å 6.188 m^2/g and 7.6, respectively.

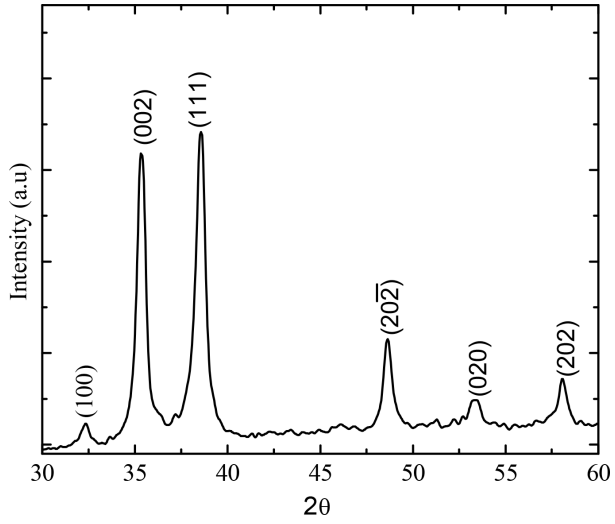

Fig. 1. XRD spectrum of as-prepared CuO NPs.

3.2. Impact of agitation time

Dependence the adsorption capacity of CuO NPs towards BB dye on the adsorption agitation time is illustrated in Fig. 3. This figure exhibits increment in the amount of BB adsorbed onto the surface of CuO NPs when adsorption shaking time is raised from 10 to 360 min and the adsorption quantity almost be constant over 360 min. Moreover, Fig. 3 shows increment in the adsorption capacity as the dye initial concentration is enhanced. Similar trends were detected by Al-Aoh et al. [38].

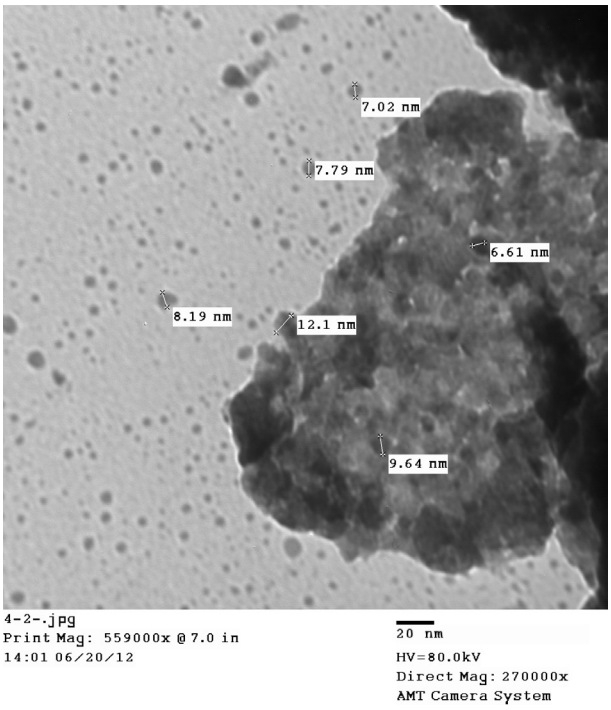

Fig. 2. TEM image of as-prepared CuO NPs.

3.3. Kinetic results analysis

The experimental data of BB adsorption kinetic onto the surface of CuO NPs were analyzed using pseudo-first order [Eq. (3)], pseudo second-order [Eq. (4)] and intraparticle diffusion [Eq. (5)] kinetic models.

The plots derived from Eqs. (3), (4) and (5) are demonstrated in Figs. 4, 5 and 6, respectively. The kinetic parameters values were calculated. These values along with the values of experimental q_{max} and association coefficients (R^2) values are listed in Tables 1 and 2.

As shown in Table 1, in case of the values pseudo second-order kinetic model, the correlation coefficients equal to the unit. It is obtained that, correlation coefficients are less than 0.93 in case of pseudo-first order kinetic model. Furthermore, the q_e values calculated using pseudo second-order model are almost similar to values of experimental q_e. The results obtained in this work indicate that second-order kinetic model is more applicable to describe adsorption of BB onto CuO NPs than first-order model. This means that adsorption of this dye by CuO NPs is second order and chemisorptions process. From these results, it is obtained an agreement of these results with these which reported in the literature [39,40].

In the case of intraparticle diffusion model (Table 2), each plot has correlation coefficients (R^2) value less than 0.84 and C value higher than zero. Furthermore, Fig. 6 illustrates that each plot over the full-time range is not linear and separated into two linear regions. This designates that the adsorption of BB on CuO NPs has been conducted by multiple steps. Similar results have been obtained by Lafi and Hafiane [41].

3.4. Impacts of initial concentration and solution temperature

Fig. 7 demonstrates the relationship between q_e (mg/g) C_i at three different temperatures (303 K, 318 K and 333 K). This figure illustrates that adsorption quantity of BB onto the surface of CuO NPs is increased with increasing initial concentration of this dye. This is because of the mass movement resistances of BB particles between solution (liquid phase)

Table 2
Parameter values of intra-particle diffusion model for BB adsorption on CuO NPs at different initial concentrations and 303 K

		Intra-particle diffusion kinetic model		
C_i (mg/L)	$q_{e,exp}$ (mg/g)	K_{dif} (mg/h$^{1/2}$g)	C	R^2
45	5.807	0.079	3.286	0.830
75	6.684	0.090	4.066	0.634
150	8.403	0.126	4.641	0.640

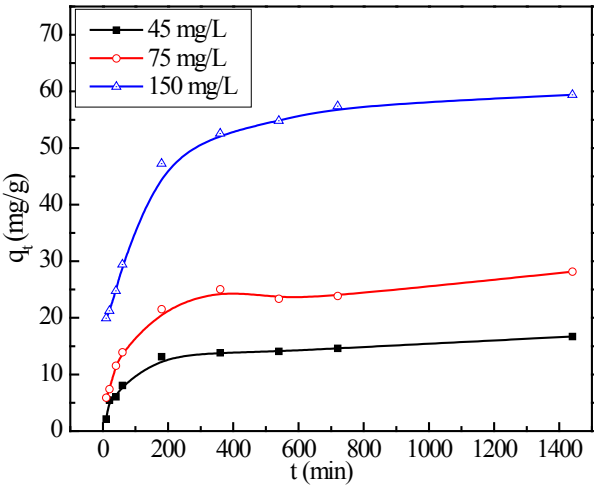

Fig. 3. Adsorption capacity of BB versus contact time on the CuO NPs.

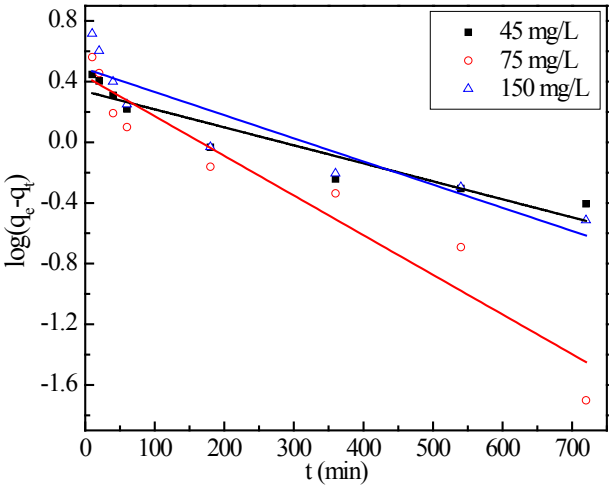

Fig. 4. Pseudo-first-order kinetic model for BB adsorption on CuO NPs.

Table 1
Pseudo-first and pseudo-second order parameters and experimental q_e values for the BB adsorption on CuO NPs at different initial concentrations and 303 K

C_o (mg/ L)	$q_{e,exp}$ (mg/g)	Pseudo-first-order kinetic model			Pseudo-second-order kinetic model			
		$q_{e,cal}$ (mg/g)	K_1 (h^{-1})	R^2	$q_{e,cal}$ (mg/g)	K_2 (g/mg·min)	R^2	Rate
45	5.807	2.17	0.003	0.876	5.82	0.0060	0.998	0.035
75	6.684	2.71	0.006	0.917	6.76	0.0085	0.999	0.057
150	8.403	3.05	0.004	0.837	8.46	0.0051	0.999	0.044

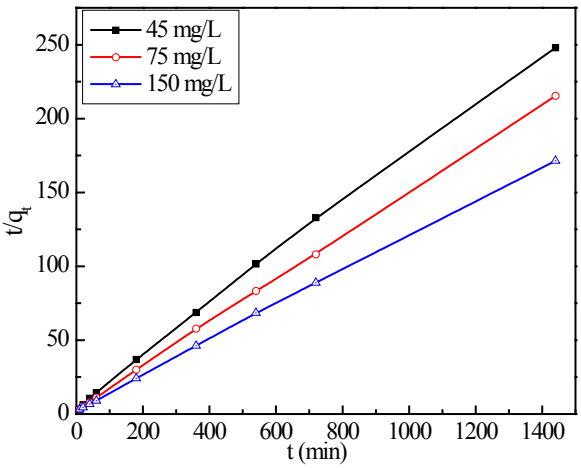

Fig. 5. Pseudo-second-order kinetic model for BB adsorption on CuO NPs.

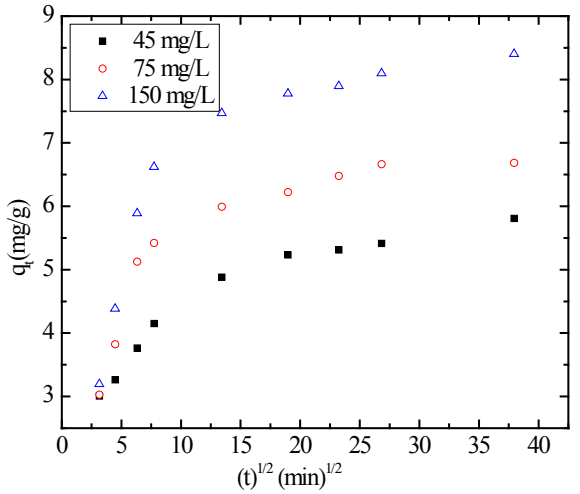

Fig. 6. Intra-particle diffusion model for BB adsorption on CuO NPs.

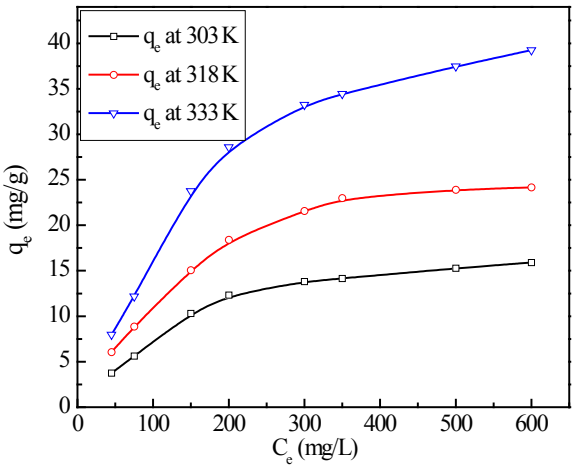

Fig. 7. Depandance of adsorption capacity on initial concentration and temperature on of BB on CuO NPs.

and adsorbent surface (solid phase) with increment the initial concentration of adsorbate [42,43]. Fig. 7 also shows that the amounts of this dye adsorbed almost become constant over 300 mg/L at each temperature. This could be due to adsorption active saturation sites when the concentration of BB increased above 300 mg/L [42,43]. Similar trends were observed in the literature [40]. Furthermore, Fig. 7 illustrates that increasing solution temperature from 303 K to 333 K leads to increment the amount of BB adsorbed onto this adsorbent surface which indicates an endothermic process. Increasing the adsorption uptake of BB by raising temperature resulted from the rising in the mobility of BB molecules [44]. Enough energy is also needed for other BB particles to uptake onto adsorption active sites [44]. It was reported in the literature that methylene blue adsorption by granular activated carbon is an endothermic process in nature [45].

3.5. Determination of isotherm parameters

The plots of Langmuir and Freundlich isotherm models in linear form are demonstrated in Figs. 8 and 9, respectively.

The calculated values of R_L were computed from values of Langmuir constant (K_L) using Eq. (8). Isotherm constants along with Values of R_L and equivalent R^2 are registered in Table 3. As seen from Table 3, values of the constant n are higher than unity and $0 < R_L < 1$.

This unity value of n indicates that adsorption of BB on CuO NPs is favorable under these experimental conditions. Figs. 8 and 9 along with values of R^2 associated with Langmuir isotherm model which is greater than that of Freundlich designate that the experimental data gives an excellent fit of the Langmuir isotherm. This means that BB adsorption on the surface of CuO NPs is a monolayer and homogeneous. It was concluded by Al-Aoh et al. [38] that adsorption data of phenolic compounds such as 4-nitophenol on commercial and fiber activated carbons provides the suitable fit of Langmuir isotherm. Moreover, Table 3 shows that adsorption capacity elevated from 20.19 to 49.84 mg/L with increasing of temperature from 303 K to 333 K. This means that adsorption of BB onto CuO NPs is endothermic

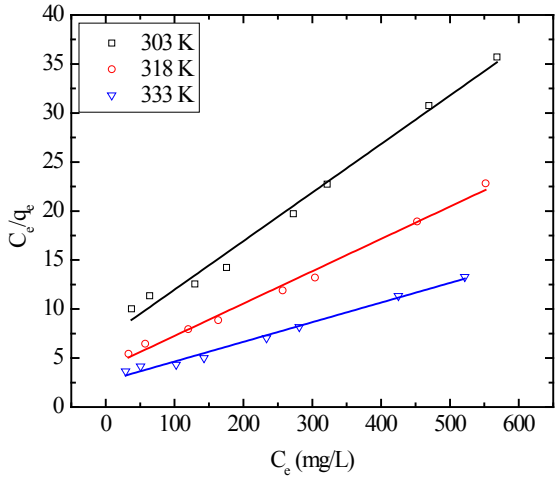

Fig. 8. Langmuir isotherm models for adsorption of BB on CuO NPs at different temperatures.

processes in nature. It also be seen from Table 3 that CuO NPs have higher adsorption capacities towards BB This indicates that CuO NPs will be a promising material for the treatment of water dyestuff pollution.

3.6. Thermodynamic analysis

The relationship between lnK_c and 1/T [Eq. (9)] for adsorption 200, 300, 500 and 600 mg/L of BB by CuO NPs at three different temperatures is illustrated in Fig. 10. The calculated ΔH° and ΔS° values are respectively from slopes and intercepts of these plots. ΔG° values were determined from values of ΔH° and ΔS° using Eq. (10). All of the thermodynamics values are registered in Table 4. As shown in this table, the ΔH° parameter has positive values which confirm that the uptake of BB by CuO NPs is endothermic in nature. These results have the same opinion with the results observed in the section which is associated to the adsorption isotherms. In addition, it can be noted from Table 4 that all of the ΔH° values are higher than the maximum values (20.9 KJ/mol) related to physisorption processes. This means that adsorption of BB by this adsorbent is chemisorptions in nature [46]. The results observed in thermodynamic section confirm the results obtained in the part of kinetic studies in terms of this adsorption is either physisorption or chemisorption processes.

Another kinetic parameter (ΔS°) has also positive values (Table 4) indicating that the randomness on the interface between solution and adsorbent is reduced by uptake of BB molecules on the adsorbent surface. Table 4 demonstrates that all of the ΔG° values are positive revealing that this type of adsorption is non-spontaneous processes. Moreover, the ΔG° values are declined by increment temperature which confirms that the main approving factor required for a significant adsorption capacity is an elevated temperature.

3.7. Impact of pH

The dependence of BB adsorption on the surface of CuO NPs (pH_{ZPC} = 7.6) on the pH of the solution is illustrated in Fig. 11. As shown in this figure, adsorption of this dye (pK_a = 3.85) decreases as solution pH is increased from 1 to 7. This can be elucidated by the fact of BB as anionic dye adsorbed on the surface of CuO NPs by electrostatic attractive forces between this anionic dye and positively charged sites exist on the adsorbent surface [47]. Since the number of positive surface charges decrease with increasing pH from 1 to 7 and then the attraction force will be reduced [47]. For this, the amount of BB adsorbed decreased with increasing pH in that range (1–7). It was reported by Iqbal and Ashiq [47] that adsorption of BB as an anionic dye on alumina is decreased when pH increased from 1 to 7.

3.8. Comparison of performance of CuO NPs with reported adsorbents

The maximum adsorption capacities of CuO NPs along with that of the other adsorbent have been used in the literatures for removal of BB from aqueous solution were sum-

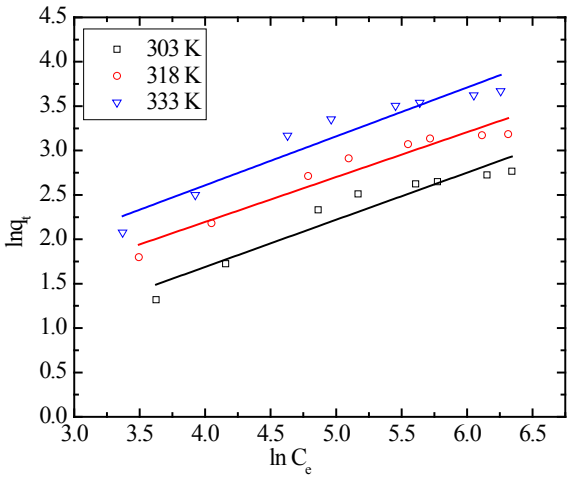

Fig. 9. Frundlish isotherm model for BB adsorption on CuO NPs at different temperatures.

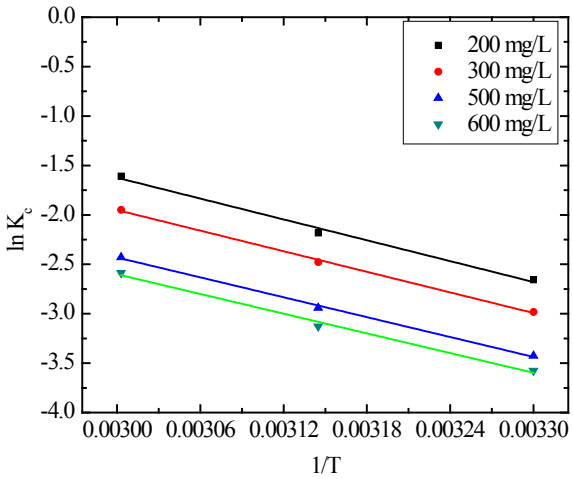

Fig. 10. lnK_c vs. 1/T for BB adsorption onto CuO NPs at different dye concentrations.

Table 3
Langmuir, Freundlich parameters and separation factors (R_L) for BB adsorption dye onto CuO NPs at three different temperatures

Temperature (K)	Langmuir isotherm				Freundlich isotherm			
	q_{max} (mg/g)	K_L (L/mg)	R_L	R^2	K_F (mg/g)(L/mg)$^{1/n}$	1/n	n	R^2
303	20.19	0.007	0.191	0.987	0.65	0.531	1.88	0.909
318	30.32	0.008	0.167	0.991	1.19	0.506	1.98	0.928
333	49.85	0.008	0.180	0.987	1.50	0.551	1.82	0.909

Table 4
Thermodynamic parameters for adsorption of BB onto CuO NPs

Concentration (mg/L)	ΔH° (kJ/mol)	ΔS° (KJ/molK)	ΔG° (KJ/mol)			
			303K	318K	333K	R^2
200	29.246	0.074	6.75	5.64	4.52	0.987
300	28.874	0.070	7.54	6.45	5.43	0.997
500	27.889	0.064	8.66	7.71	6.76	0.997
600	27.630	0.061	9.07	8.15	7.23	0.987

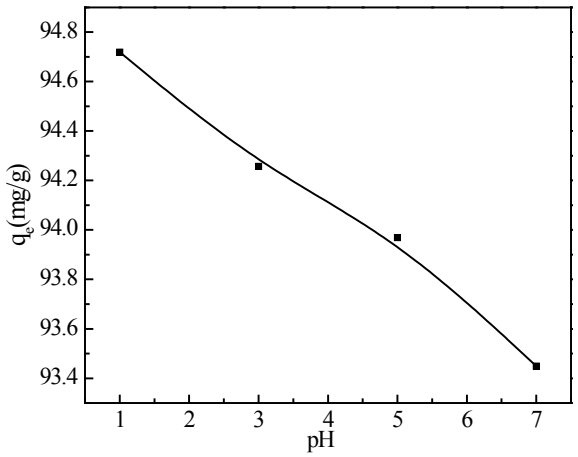

Fig. 11. Effect of pH on BB adsorption by CuO NPs.

Table 5
Comparison of adsorption capacity of CuO NPs used as adsorbent in this study with other adsorbents towards BB

Adsorbent	q_{max} (mg/g)		Sources
α-chitin	22.72		(Dhananasekaran et al. 2016) [27]
Polymeric gels	2.99		(Malana et al. 2010) [28]
Mesoporous hybrid gel	17.69	298 K	(You et al. 2016) [29]
	17.42	323 K	
	18.43	348 K	
Alumina	6.36	298 K	(Iqbal and Ashiq. 2010) [47]
	5.70	303 K	
	5.64	308 K	
	4.56	313 K	
	2.92	318 K	
Sorel's cement NPs	16.39		(El-Gamal et al. 2015) [48]
Activated carbon	1.89		(Dada et al. 2012) [49]
Magnetic chitosan-graphene oxide composite	28		(Sohni et al. 2017) [50]
CuO NPs	20.19	303 K	Present study
	30.32	318 K	
	49.85	333 K	

marized in Table 5 to demonstrate the importance of CuO NPs used in this work comparing to others. This table indicates that CuO NPs have adsorption performance higher than that of other which indicates that this type of NPs will met a significant interesting in the case of water purification activities.

4. Conclusions

Isotherms, kinetic and thermodynamic constants of BB adsorption onto CuO NPs along with the effects of experimental factors were examined. The obtained results demonstrate that BB initial concentration, agitation time and temperature have positive effects on the adsorption capacity but pH solution has a negative impact. Langmuir isotherm model was obtained to be the best model to describe the isotherm experimental data, designating that BB adsorption onto CuO NPs is a homogeneous and monolayer. The greatest-fit adsorption kinetic has been attained with the second-order kinetic model. The results of thermodynamic suggest that BB adsorption onto this adsorbent is un-spontaneous and endothermic processes. Both of kinetics and thermodynamic studies confirm that BB adsorption onto CuO NPs is chemisorption.

Acknowledgement

The authors extend their appreciation to the Deanship of Scientific Research at Tabuk University for funding the work through the research group Project No. S-90-1437H.

References

[1] N.M. Shaalan, M. Rashad, A.H. Moharram, M.A. Abdel-Rahim, Promising methane gas sensor synthesized by microwave-assisted Co_3O_4 nanoparticles, Mater. Sci. Semicond. Process., 46 (2016) 1–5.
[2] N.M. Shaalan, M. Rashad, M.A. Abdel-Rahim, Repeatability of indium oxide gas sensors for detecting methane at low temperature, Mater. Sci. Semicond. Process., 56 (2016) 260–264.
[3] M. Rashad, Taymour A. Hamdalla, S.E. Al Garni, A.A.A. Darwish, S.M. Seleim, Optical and electrical behaviors in NiO/xFe_2O_3 nanoparticles synthesized by microwave irradiation method, Optic. Mater., 75 (2018) 869–874.
[4] N.M. Shaalan, M. Rashad, M.A. Abdel-Rahim, CuO nanoparticles synthesized by microwave-assisted method for methane sensing, Opt. Quant. Electron., 48 (2016) 531.
[5] H. Wang, J.-Z. Xu, J.-J. Zhu, H.-Y. Chen, Preparation of CuO nanoparticles by microwave irradiation, J. Crystal Growth, 244 (2002) 88–94.

[6] A.A. Hendi, M. Rashad, Photo-induced changes in nano-copper oxide for optoelectronic applications, Physica B, 538 (2018) 185–190.
[7] Y. Aparna, K.V. Enkateswara Rao, P. Srinivasa Subbarao, Synthesis and characterization of CuO nano particles by novel sol-gel method, 2nd International Conference on Environment Science and Biotechnology, 48 (2012) 156–160.
[8] S. Srivastava, M. Kumar, A. Agrawal, S.K. Dwivedi, Synthesis and characterisation of copper oxide nanoparticles, J. Appl. Phys., 5 (2013) 61–65.
[9] A. Asha Radhakrishnan, B. Baskaran Beena, Structural and optical absorption analysis of CuO nanoparticles, Indian J. Adv. Chem. Sci., 2 (2014) 158–161.
[10] P. Mallick, S. Sahu, Structure, microstructure and optical absorption analysis of CuO nanoparticles synthesized by sol-gel route, Nanosci. Nanotechnol., 2 (2012) 71–74.
[11] A. Fakhri, Adsorption characteristics of graphene oxide as a solid adsorbent for aniline removal from aqueous solutions: Kinetics, thermodynamics and mechanism studies, J. Saudi Chem. Soc., 21 (2017) S52–S57.
[12] S. Reddy, B.E. Kumara Swamy, H. Jayadevappa, CuO nanoparticle sensor for the electrochemical determination of dopamine, Electrochim. Acta., 61 (2012) 78–86.
[13] N. Bouazizi, R. Bargougui, A. Oueslati, R. Benslama, Effect of synthesis time on structural, optical and electrical properties of CuO nanoparticles synthesized by reflux condensation method, Adv. Mater. Lett., 6 (2015) 158–164.
[14] A. Eslami, N.M. Juibari, S.G. Hosseini, M. Abbasi, Synthesis and characterization of CuO nanoparticles by the chemical liquid deposition method and investigation of its catalytic effect on the thermal decomposition of ammonium perchlorate, Centr. Europ. J. Energ. Mater., 14 (2017) 152–168.
[15] M. Rashad, N.M. Shaalan, A.M. Abd-Elnaiem, Degradation enhancement of methylene blue on ZnO nanocombs synthesized by thermal evaporation technique, Desal. Water Treat., 57(54) (2016) 26267–26273.
[16] X. Liu, Z. Li, Q. Zhang, F. Li, T. Kong, CuO nanowires prepared via a facile solution route and their photocatalytic property, Mater. Lett., 72 (2012) 49–52.
[17] H.S. Devi, T.D. Singh, Synthesis of copper oxide nanoparticles by a novel method and its application in the degradation of methyl orange, Adv. Electron. Elect. Eng., 4 (2014) 83–88.
[18] M.A. Bhosale, S.C. Karekar, B.M. Bhanage, Room temperature synthesis of copper oxide nanoparticles: morphological evaluation and their catalytic applications for degradation of dyes and C–N bond formation reaction, Chemistry Select, 1 (2016) 6297–6307.
[19] A. Nezamzadeh-Ejhieh, H. Zabihi-Mobarakeh, Heterogeneous photodecolorization of mixture of methylene blue and Bromophenol blue using CuO-nano-clinoptilolite, J. Ind. Eng. Chem., 20 (2014) 1421–1431.
[20] G. Mustafa, H. Tahir, M. Sultan, N. Akhtar, Synthesis and characterization of cupric oxide (CuO) nanoparticles and their application for the removal of dyes, Afric. J. Biotechnol., 12 (2013) 6650–6660.
[21] A. Shiue, C.-M. Ma, R.-T. Ruan, C.-T. Chang, Adsorption kinetics and isotherms for the removal methyl orange from wastewaters using copper oxide catalyst prepared by the waste printed circuit boards, Environ. Res., 22 (2012) 209–215.
[22] J. Yang, S. Cui, J.-q. Qiao, H.-z. Lian, The photocatalytic dehalogenation of chlorhenols and bromophenols by cobalt doped nano TiO_2, J. Molec. Catal. A: Chemical, 395 (2014) 42–51.
[23] Y. Lu, Y. Wang, X. Zhu, The removal of bromphenol blue from water by solvent sublation, Separ. Sci. Technol., 36 (2011) 3763–3776.
[24] Y. Lu, Y. Wang, X. Zhu. The removal of bromophenol blue from water by solvent solution, Separ. Sci. Technol., 36 (2001) 3763–3776.
[25] R. Azmat, Z. Khalid, M. Haroon, K. B. Mehar. Spectral analysis of catalytic oxidation and degradation of bromophenol blue at low pH with potassium dichromate, Adv. Nat. Sci., 6 (2013) 38–43.
[26] N.K. Temel, R. Gürkan, F. Ayan, Photocatalytic TiO_2-catalyzed degradation of bromophenol blue-mediated Mo(VI)-peroxo complexes in the presence of SDS, Desal. Water Treat., 57 (2016) 21083–21090.
[27] S. Dhananasekaran, R. Palanivel, S. Pappu, Adsorption of methylene blue, bromophenol blue, and coomassie brilliant blue by a-chitin nanoparticles, J. Adv. Res., 7 (2016) 113–124.
[28] M.A. Malana, S. Ijaz, M.N. Ashiq, Removal of various dyes from aqueous media onto polymeric gels by adsorption process: Their kinetics and thermodynamics, Desalination, 263 (2010) 249–257.
[29] L. You, Z. Wu, T. Kim, K. Lee, Kinetics and thermodynamics of bromophenol blue adsorption by a mesoporous hybrid gel derived from tetraethoxysilane and bis (trimethoxysilyl) hexane, J. Colloid Interf. Sci., 300 (2006) 526–535.
[30] J. Liu, S. Yao, L. Wang, W. Zhu, J. Xu, H. Song, Adsorption of bromophenol blue from aqueous samples by novel supported ionic liquids, J. Chem. Technol. Biotechnol., 89 (2014) 230–238.
[31] M. Rashad, A.M. Ali, M.I. Sayyed, I.V. Kityk, Photoluminescence features of magnetic nano-metric metal oxides, J. Mater. Sci. Mater. Electron. (2018).
[32] M. Rashad, M. Rüsing, G. Berth, K. Lischka, A. Pawlis, CuO and Co_3O_4 nanoparticles: synthesis, characterizations, and Raman spectroscopy, J. Nanomater., Vol. 2013, 1–6 Article ID 714853, 6 pages.
[33] S.K. Theydan, M.J. Ahmed, Adsorption of methylene blue onto biomass-based activated carbon by $FeCl_3$ activation: Equilibrium, kinetics, and thermodynamic studies, J. Anal. Appl. Pyrol., 97 (2012) 116–122.
[34] H.A. Al-Aoh, adsorption performance of nickel oxide nanoparticles (NiO NPs) towards bromophenol blue due (BB), Desal. Water Treat., 110 (2018) 229–238.
[35] F. Ahmad, W.M.A.W. Daud, M.A. Ahmad, R. Radzi, Using cocoa (The obroma cacao) shell-based activated carbon to remove 4-nitrophenol from aqueous solution: Kinetics and equilibrium studies, Chem. Eng. J., 178 (2011) 461–467.
[36] G. Atun, G. Hisarli, W.S. Sheldrick, M. Muhlerler, Adsorptive removal of methylene blue from colored effluents on fullers earth, J. Colloid Interf. Sci., 261 (2003) 32–39.
[37] A.H. Moharram, S.A. Mansour, M.A. Hussein, M. Rashad, Direct precipitation and characterization of ZnO nanoparticles, J. Nanomater., vol. 2014, Article ID 716210.
[38] Hatem. A. Al-Aoh, M.J. Maah, Rosiyah. Yahya, M.R. Bin Abas, Isotherms, kinetics and thermodynamics of 4-nitrophenol adsorption on fiber-based activated carbon from coconut husks prepared under optimized conditions, Asian J. Chem., 25 (2013) 9573–9581.
[39] S.F. Soares, T.R. Simões, T. Trindade, A.L. Daniel-da-Silva, Highly efficient removal of dye from water using magnetic carrageenan/silica hybrid nano-adsorbents, Water Air Soil Pollut., 228 (2017) 87.
[40] H.A. Al-Aoh, M.J. Maah, R. Yahya, M.R. Bin Abas, A comparative investigation on adsorption performances of activated carbon prepared from coconut husk fiber and commercial activated carbon for acid red 27 dye, Asian J. Chem., 25 (2013) 9582–9590.
[41] R. Lafi, A. Hafiane, Removal of methyl orange (MO) from aqueous solution using cationic surfactants modified coffee waste (MCWs), J. Taiwan Inst. Chem. Eng., 58 (2016) 424–433.
[42] Q. Baocheng, Z. Jiti, X. Xuemin, Z. Chunli, Z. Hongxia, Z. Xiaobai, Adsorption behavior of Azo Dye C. I. Acid Red 14 in aqueous solution on surface soils, J. Environ Sci., 20 (2008) 704–709.
[43] V.K. Gupta, B. Guptaa, A. Rastogi, S. Agarwal, A. Nayak, A comparative investigation on adsorption performances of mesoporous activated carbon prepared from waste rubber tire and activated carbon for a hazardous azo dye Acid Blue 113, J. Hazard. Mater., 186 (2011) 891–901.
[44] B.H. Hameed, A.A. Ahmad, Batch adsorption of methylene blue from aqueous solution by garlic peel, an agricultural waste biomass, J. Hazard. Mater., 164 (2009) 870–875.

[45] H.A. Al-Aoh, R. Yahya, M.J. Maah, M.R. Bin Abas, Adsorption of methylene blue on activated carbon fiber prepared from coconut husk: isotherm, kinetics and thermodynamics studies, Desal. Water Treat., 52 (2014) 6720–6732.
[46] A. Kurniawan, S. Ismadji, Potential utilization of Jatropha curcas L. Press-cake residue as new precursor for activated carbon preparation: Application in methylene blue removal from aqueous solution, J. Taiwan Inst. Chem. Eng., 42 (2011) 826–836.
[47] M.J. Iqbal, M.N. Ashiq, Thermodynamics and kinetics of adsorption of dyes from aqueous media onto alumina, J. Chem. Soc. Pak., 32 (2010) 419–428.
[48] S.M.A. El-Gamal, M.S. Amin, M.A. Ahmed, Removal of methyl orange and bromophenol blue dyes from aqueous solution using Sorel's cement nanoparticles, JECE., 3 (2015) 1702–1712.
[49] A.O. Dada, A.A. Inyinbor, A.P. Oluyori, Comparative adsorption of dyes unto activated carbon prepared from maize stems and sugar cane stems, IOSR-JAC., 2 (2012) 38–43.
[50] S. Sohni, K. Gul, F. Ahmad, I. Ahmad, A. Khan, N. Khan, S.B. Khan, Highly efficient removal of acid red-17 and bromophenol blue dyes from industrial wastewater using graphene oxide functionalized magnetic chitosan composite, Polym. Comp., (2017) DOI 10.1002/pc.24349.